Long-term deformation analysis of Masjed-Soleyman rockfill dam (Iran): results based on terrestrial geodetic data

Lotfollah Emadali[1]*, Mahdi Motagh[2,3]

[1]Department of Civil Engineering, Engineering Faculty, Khatam al Anbia Behbahan Technical University, Behbahan, Iran

[2]GFZ German Research Center for Geosciences, Department of Geodesy and Remote Sensing, 14473 Potsdam, Germany

[3]Institute for Photogrammetry and Geo-Information, Leibniz Universität Hannover, Hannover, Germany

ABSTRACT

In this research, the post-construction movement of the Masjed-Soleyman dam in southwest Iran was investigated using 15 years of terrestrial geodetic measurements between 2000 and 2015. The stability analysis of the dam body was assessed using the settlement index (SI) criterion. Moreover, a relaxation model was developed for the prediction of deformation in time. The results show that between 2000 and 2015, the middle part of the crest (382.0 m) experienced the highest settlement of about 3.5 m, equivalent to about 2 % of the dam height. For the downstream slope, the middle part of the dam body at 350 m shows the maximum cumulative settlement of about 1.2 m in 15 years. The maximum cumulative horizontal displacement belonged to the middle part of the downstream slope, reaching about 1.4 m. The points located near the side staddles experienced smaller horizontal and vertical movements; the maximum cumulative vertical and horizontal displacements for side points of the crest were about 1 m and 0.7 m, respectively. The stability analysis using the settlement index shows that the points on the downstream embankment have the normal values of settlement index (i.e., 0.02) during the examination, and thus, their settlement could be considered as creep or secondary consolidation. However, the points located in the middle part of the crest exhibit a settlement index that exceeds the instability threshold. The relaxation model that developed in this study suggests that except for some points located on the bottom part of the downstream slope of the embankment, the settlement of the other points will continue for the next few years, even after 30 years of the dam operation. However, the maximum rate of deformations would decrease and reach from 25 cm/yr for the first 15 years of dam operation to 10 cm/yr in the 30th year of operation.

1. Introduction

Dams are important structural barriers that have several functions in water reservoirs, including storing drinking water, flood control, agricultural irrigation, and power generation. They are subject to internal (e.g., weight of the dam body, reservoir water pressure) and external loads (e.g., earthquake, changes of temperature) that cause deformation. This deformation needs to be monitored from construction until filling the reservoir, as well as during the operation, to ensure that the dam operates within safety limits (Gikas, Vassilis, sakellariou, & Michael, 2008) . The

monitoring methods for evaluating dam safety can be divided into two categories: (1) non-geodetic (geotechnical) methods, (2) geodetic methods. Geotechnical methods are based on installing a set of mechanical tools such as strain gauges or extensometers, inclinometers, inverted pendulum, and other similar devices inside the dam structure (Dunnicliff & John, 1988). Geodetic techniques include either terrestrial surveys such as classical or GPS measurements (Radhakrishnan & Nisha, 2014) or remote sensing methods like SAR Interferometry (Hanssen, 2001) (Massonnet & Feigl, 1998) (Emadali, L, Motagh, M, &

Haghshenas, M, 2017) (Shamshiri, et al., 2014) (Milillo, et al., 2016).

In this paper, the post-construction behavior of the Masjed-Soleyman dam in southwest Iran (Figure 1) is investigated using 15 consecutive surveying measurements from December 2000 to May 2015. This dam is a large earth core rockfill dam (ECRD) with a large size vertical clay core constructed in 2000. The detailed information about the geometry, construction, and filling of the reservoir, as well as the investigation carried out on contemporary deformation using SAR interferometry, are given in (Emadali, L, Motagh, M, & Haghshenas, M, 2017). The cross-section of the dam that includes a vertical clay core, transition (filter) zones at two sides of the core, and

upstream and downstream sand-gravel shells is shown in Figure 1c. The technical specifications of the Masjed-Soleyman dam are summarized in Table 1 (F, 2004).

Table 1. Technical specifications of the Masjed-Soleyman dam

Height from foundation	177 m	Slope of upstream	1 / 2
Crest length	497 m	Slope of downstream	1 / 1.75
Width from toe to toe	780 m	Power station	2000 MWatts
Width of crest	15 m	Capacity of spillway	21700 m³/sec
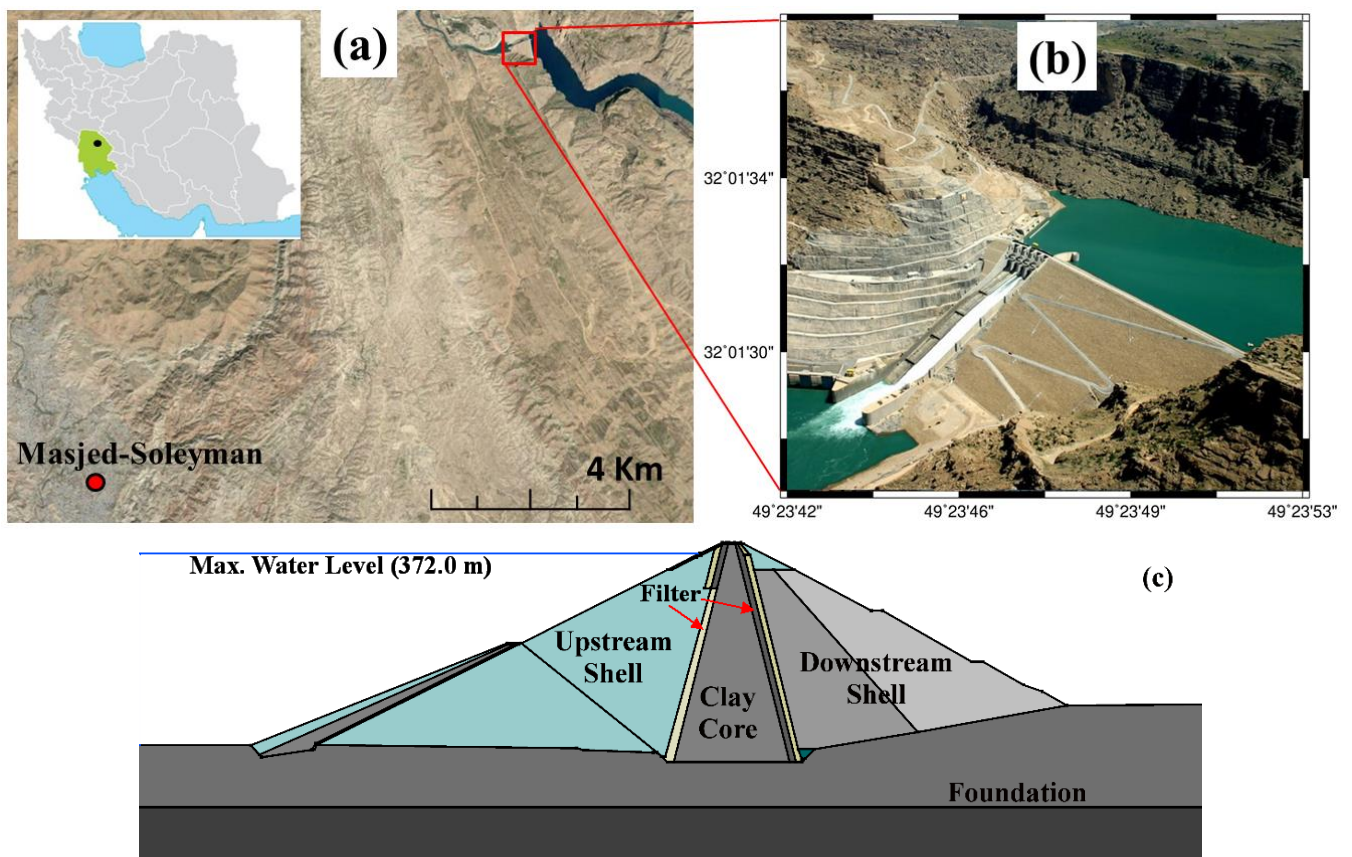
Figure 1. The Masjed-Soleyman dam; (a) Location of the dam in the Khuzestan province, Southwest of Iran; The black circle shows the location of the dam; (b) Embankment, spillway, and the water reservoir of the dam; (c) Cross-section of the dam at the chainage of 260 m including foundation, clay core, filters, upstream and downstream shells.

Figure 2 shows some ground pictures of the damage and destruction that occurred on the crest and embankment of the Masjed-Soleyman dam from its deformation. Settlement of the crest, especially in the middle part of the dam, creep of upstream and downstream rock-filled shells, cross and

longitudinal cracks along the crest are abundantly seen in different parts of the crest and embankment of the dam. In the following, we present the results of terrestrial geodetic surveys performed between 2000 and 2015 to monitor and assess the vertical and horizontal deformation of the dam.
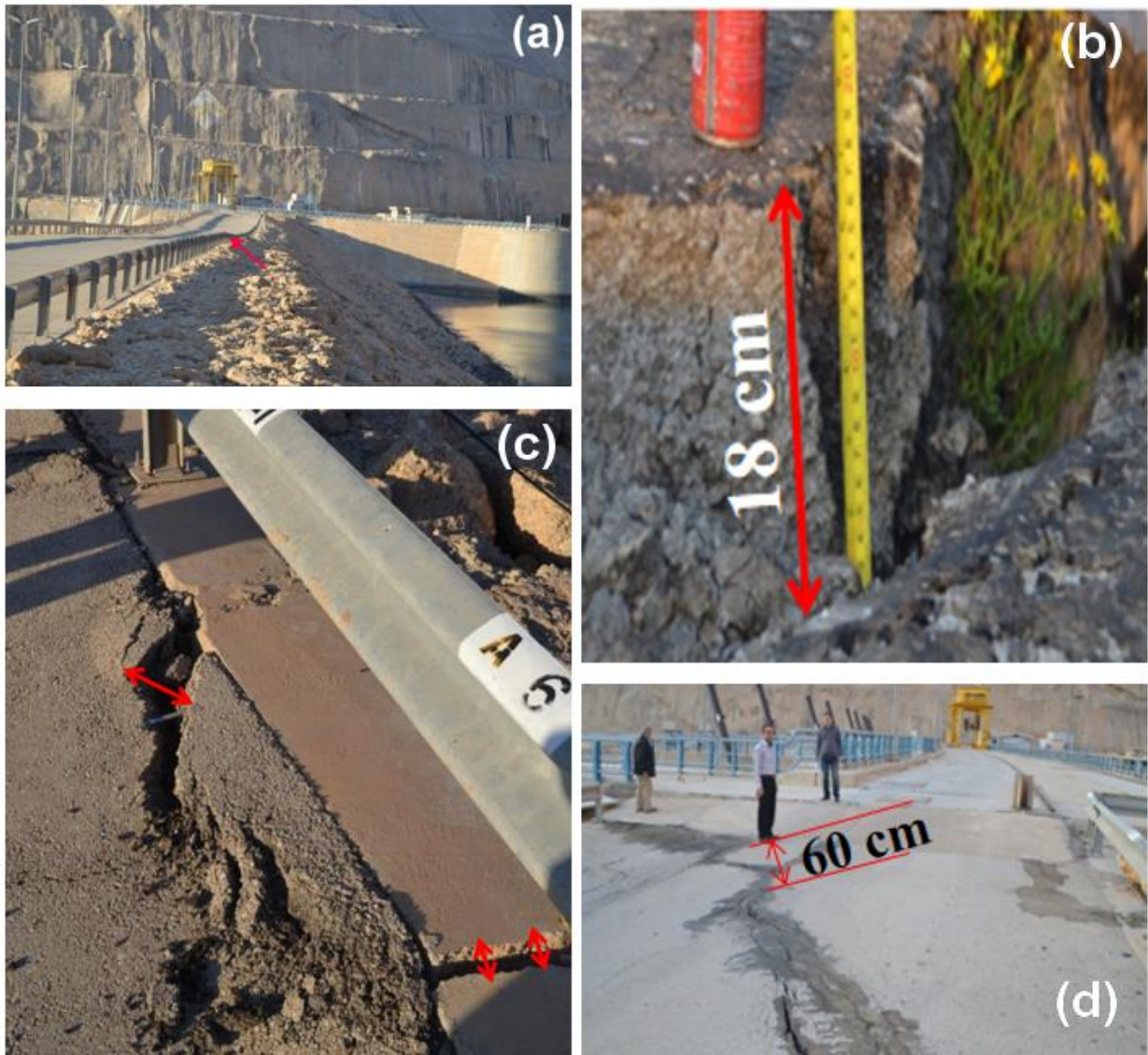
Figure 2. Exemplary ground pictures of damages and cracks of the Masjed-Soleyman dam. (a) Settlement of crest and creep of the upstream embankment, (b) cross cracks along the crest, (c) longitudinal cracks of the crest, (d) vertical displacement and cracks at the crest as a result of the settlement of earth body of dam with respect to the concrete spillway.

2. Data and methods

2.1. Terrestrial Surveying

Following the construction of the Masjed-Soleyman dam, a geodetic network was created on and around the dam to measure the horizontal and vertical displacement of target points installed on the dam. The monitoring system includes three sub-networks as (1) two dimensional (2D) network of reference points (off-dam), (2) 2D network of target points established on the dam body (on-dam), and (3) a leveling network. Also, two 3D networks were created to monitor the spillway, consisting of 10 target points, and galleries, consisting of 10 target points). All the points of geodetic networks were constructed as concrete pillars with a forced centering system to minimize the centering errors of surveying instruments (Figure 3c).

The off-dam network of the Masjed-Soleyman dam consists of 13 reference points that spread over an area of about 4 km² around the dam site. Twenty-six control stations that were established on the crest and the downstream slope make the on-dam network for monitoring the horizontal and vertical movements of the dam (Figure 3). All points of this network have been observed from 6 off-dam pillars in two separate steps. At first, the horizontal position of points was determined by a total station, and then, the height of points was measured by a high-precision digital level (See Tab. 2 for the specification of instruments). Generally, observations of these networks, including lengths, angles, and height differences between target and reference points were measured in 15 consecutive periods from December 2001 to May 2015, but the lapse time between consecutive measurements is not equal (Baarda, 1968).

All slope distances, horizontal directions, and vertical angles have been measured in 4 acceptable sets. Slope distance measurements were carried out reciprocally for the off-dam network points, whereas the distances between reference points and target points were measured as one-way. In order to apply the atmospheric corrections to the observed distances, atmospheric parameters, including the wet and dry temperatures and air pressure, were measured during the observation process.

Generally, geodetic measurements were made every six months; however, in some cases, the time interval between observations was increased to 1 year or more. Measurement procedure was nearly uniform (usually the same instruments, similar techniques, a fixed surveying team, etc.); thus, the data are completely homogeneous and of the same accuracy (Rahimi, 2003).

Table 2. Surveying instruments used for observation of geodetic network

Instruments	Manufacturer	Accuracy	Accessories
Total Station TCA2003	Leica	1mm+1ppm & 0.5 Sec.	Wet and Dry Thermometer, Barometers, Precise Reflectors And Targets
Digital Level DNA03	Leica	0.3mm/Km	Barcode Invar Staffs (3m and 92cm)
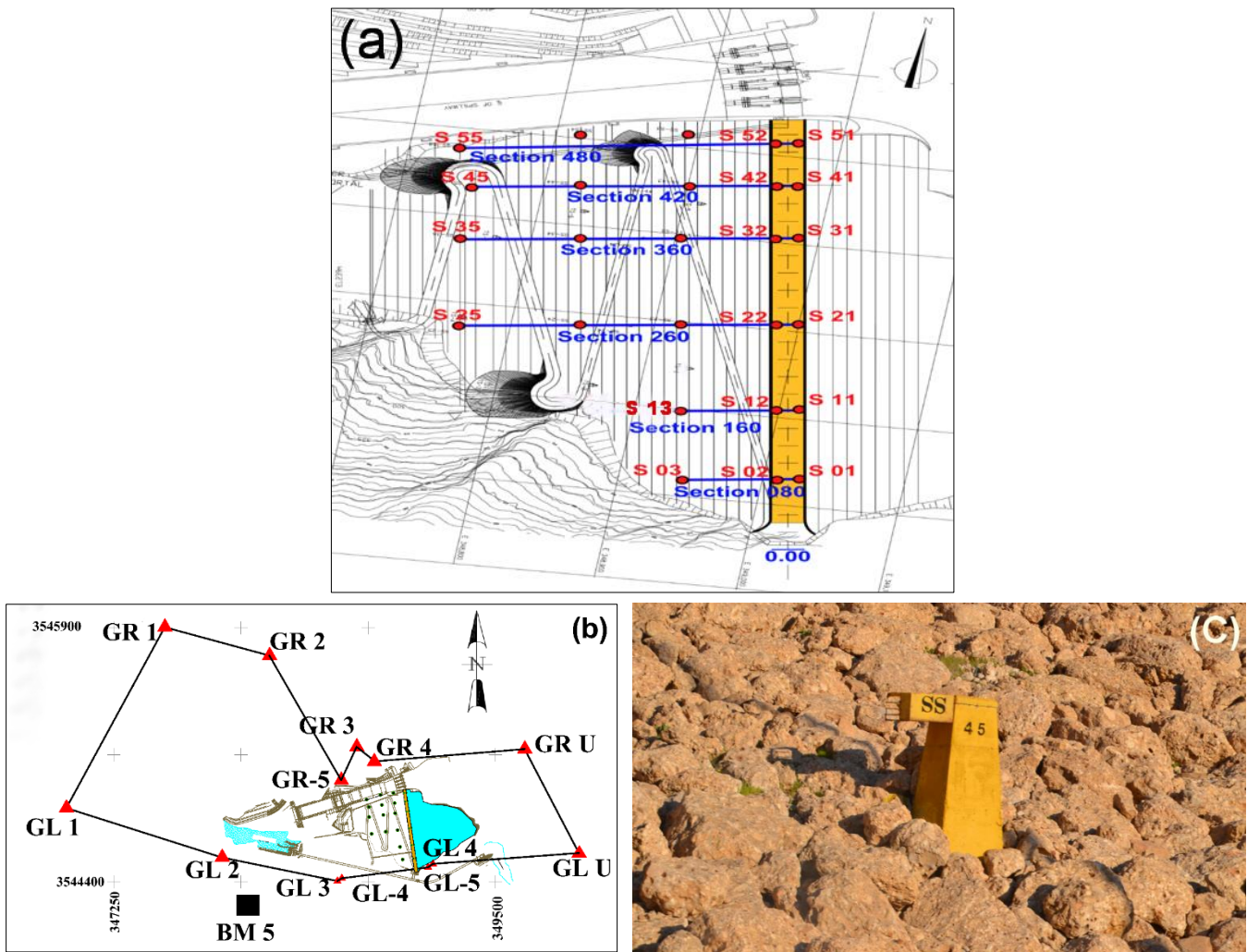
Figure 3. (a) On-dam geodetic network of the Masjed-Soleyman dam. Twenty-six target points were installed on the crest and downstream slope of the dam. The blue lines show the cross-sections of the dam. (b) Off-dam and On-dam geodetic networks: GR3 and BM5 are the fixed points for horizontal and vertical measurements, respectively. (c) Concrete pillar of the geodetic networks established on the dam body.

2.2. Adjustment of the geodetic networks

In order to determine the horizontal and vertical displacements, the observations for horizontal displacement detection (horizontal directions and distances) and the leveling measurements were adjusted separately. Since the number of observations in each measurement campaign was more than the unknowns (coordinates of points), the least square method was used to estimate the unknowns. First, the off-dam network was adjusted by the inner-constraint method (e.g., Vaniček et al., 1986) to determine the stable points (GR3 and GL4 in Figure 3b). Then, the on-dam network was adjusted by the minimum constraint method with this assumption that the point (GR3) and a direction (GR3 to GL4) were fixed (Figure 3b). The maximum value for the semi-major axis of the error ellipses was 2.4 mm for the Reference Point GL1. Also, the internal reliability based on the method of Baarda (1968) was utilized to show the ability of the geodetic networks for blunder detection and network resistance against undetectable probable observations errors (Kalkan, 2014).

For the leveling network, the Benchmark BM5 was set as the fixed point for the minimum constraint adjustment of the target points (Vanicek & Krakiwsky, 1986). In this network, the maximum standard deviation of the heights of the points was 0.8 mm for all the target points located on upstream and downstream edges of the crest (Figure 3b).

The type and number of observations for off-dam, on-dam, and leveling networks for the last period (15th period) of measurements are summarized in table 3. The maximum horizontal and vertical displacements of the dam at the 15th period (the last observation) relative to the 14th period and also the values of cumulative displacements from the first series of observations in 2000 to the last session of observation in 2015 are summarized in Tables 4 and 5. More details are presented in section 4.

Table 3. Observations of monitoring networks of the Masjed-Soleyman dam

Network	Observations				Max. Semi-Major Axis of Error Ellipses (mm)	Degree of freedom
	Slope Distance	Horizontal Direction & RMSE	Vertical Angle & RMSE	Height Difference & SD (mm)		
Off-dam	47	96 (0.26)	96 (0.41)	-	2.4	107
On-dam	88	94 (0.22)	94 (0.35)	-	1.5	126
Levelling	-	-	-	29 (0.8)	-	-

Table 4. Maximum horizontal and vertical displacements of the dam from 2000 until 2015
(15th period relative to the first period)

Network	Max. Horizontal Displacements (mm)		Max. Vertical Displacements (mm)	
	Point Name	D (mm)	Point Name	ΔZ (mm)
On-dam horizontal network	S 23	1410.7	***	***
Leveling network	****	****	S 21	-3525.96

Table 5. Maximum horizontal and vertical displacements of the dam from Feb. 2014 until May 2015
(15th period relative to 14th period)

Network	Max. Horizontal Displacements(mm)		Max. Vertical Displacements (mm)	
	Point Name	D (mm)	Point Name	ΔZ (mm)
On-dam horizontal network	S 23	72.76	***	***
Leveling network	****	****	S 21	-165.2

2.3. Settlement Index

Steady-state loading refers to the situation where there is no change in reservoir level and, therefore, no change in the external load on the dam. It may be expected that some settlement will continue to occur even many years after the completion of construction owing to the secondary consolidation of the core and creep of the more granular shoulder fill.

In order to quantify the movements associated with the long-term steady-state loading, the crest settlements were evaluated using the dimensionless quantity of settlement index (S_I) (Clements & Ronald , 1984), which is analogous to the coefficient of secondary consolidation. S_I reflecting the average settlement of a point located on an earthfill or rockfill dam during a certain interval normalized to the height of the dam at the specific point (Pytharouli, Stella , & Stathis , 2009):

$$S_I = \frac{s}{1000 \times H \times \log\left(\frac{t_2}{t_1}\right)} \qquad (1)$$

Where:

s (mm) is the crest settlement between two different measurement periods t_1 and t_2 for each object point installed on the dam's embankment, H (m) is the height of points relative to the foundation level. Expressed that if the value of the parameter S_I is greater than 0.02, the crest settlement is attributed to mechanisms other than creep or secondary consolidation requiring further investigation to be conducted.

The annual rate of settlement (S_a) was also used to assess the deformations of the crest and downstream embankment of the dam (Michalis & Pytharouli, 2016):

$$S_a = \left(\frac{S_{ii} - S_i}{H}\right) \times 100 \qquad (2)$$

Where S_{ii} and S_i are consecutive yearly settlement measurements, and H is the height from the foundation level at each crest control point. For each point with the value of S_a equal or less than 0.02% of the height of the dam, it is considered that the point has normal subsidence, and the dam is stabilized (Dascal, 1987). Considering the effect of settlement caused by consolidation, for the points with the greater height of embankment, it is expected that the greater settlements would be seen.

2.4. Relaxation Model

We analyzed and modeled the temporal and spatial evolution of surface deformation of the Masjed-Soleyman dam after the end of construction using a relaxation process with three characteristic times: (1) after the construction (short term), (2) after water impoundment of the reservoir (intermediate-term), and (3) long-time relaxation during the operation of the dam (long term). By definition, Relaxation time is defined as the time required for a viscous substance to recover from shearing stress after the flow has ceased.

We assumed that the short relaxation time might be caused by pore water pressure developed in the dam body during and immediately after the end of construction, i.e., the primary consolidation. The intermediate relaxation time was corresponding to the time duration when the reservoir of the dam was filled. The long relaxation time was corresponding to the secondary consolidation of materials that led to plastic deformation on the dam body.

To explain the temporal behavior of deformation at target points, the following model with three exponential terms, corresponding to three specified relaxation times, were selected from a variety of possible models:

$$dz(t_j) = a + \sum_{i=1}^{3} b_i \exp\left(-(t_j - t_0)/\tau_i\right) \qquad (3)$$

Where:

$dz(t_j)$: the displacement in the z-direction (settlement) at the time t_j,

a : the final displacement at the time t_∞,

b_i : the amplitude of the deformation signal,

t_0 : Reference time, when the construction was ended

t_j : time of measurements with respect to the t_0

τ_i : Relaxation time;

The criteria for selecting a model for each point were the RMSE and R-Square values. R-square is a measure of the goodness of fit of the trend-line to the data. In other words, R^2 is a number that indicates the proportion of the variance in the dependent variable that is predictable from the independent variable. A value of 1 is a perfect fit. Thus, the best model of relaxation time is a model with the least RMSE and R-square value as closely as to 1 (Savage & Svarc, 2009).

According to this model, 15 series of surveying measurements were utilized to estimate the seven coefficients of the model based on the least square adjustment. At first, the primary values were selected for three coefficients of relaxation time. These primary values were determined based on the three steps of dam operation:

• The first relaxation time starts with the end of construction or the step of primary compaction, which takes a duration time of about 6 to 10 months (Dascal, 1987). For this analysis, the first relaxation time was set to 180 days.

• The second relaxation time is related to the time of filling the dam reservoir. This step has occupied a three-year period (Figure 2). Thus, the primary value of 1095 days was considered for this parameter.

• The third relaxation parameter is concerned with the secondary consolidation that happens in adhesive soils such as clay in the core of the dam during the dam operation. The primary value of this parameter was considered according to the rate of the height differences of each geodetic point during 15 series of data accumulation.

According to these three main parameters (τ_1, τ_2, τ_3) and the primary values considered for other unknowns (a, b_1, b_2, b_3), the final values of unknowns were estimated by the non-linear least square method, and then, the settlement model was determined for each geodetic point of the on-dam network. The results would be discussed in section 4.3.

3. Deformation Analysis
3.1. Vertical Displacement

Table 6 shows the cumulative horizontal and vertical displacements of target points located on the crest and downstream slope of the dam (On-dam network) between December 2000 and May 2015. As Table and Figure 4 show, the maximum vertical displacement of the points

belongs to points S21 and S22, located in the middle part of the crest (section 260 m in Figure 3) with the magnitude being about 3500 and 3300 mm, respectively. This section is in the middle part of the dam influenced by the most water pressure of the dam reservoir. It also has the highest elevation of the embankment that influence deformation.

Figure 4 illustrates the time-series of the settlement of the points listed in Table 6 (On-dam network). The reference date is the date of the first series of terrestrial measurements of the network that was performed shortly after the first water impoundment of the dam. As seen, the settlement of the dam body continues with different rates at all target points (see 4.3). In the middle part of the dam body (sections 260 and 360 in Figure 3c), the settlement has a greater rate concerning the corner sections. Also, the settlement decreases from the crest toward the points located on the bottom of the downstream embankment (points in the level of 270 m). From geodetic observations, it seems that the settlement of the dam body has asymmetric structure so that the points located on the corresponding sections of the dam (sections 80 & 480 m, sections 160 & 420 m, sections 260 & 360 m) have the same pattern of settlement (Pagano, L, Desideri, A, & Vinale, F, 1998).

As is clear from Figure 4, the right and left sections have symmetry in their settlement patterns. In other words, the magnitude of the settlement of points located in section 80 and 480 (see Figure 3a) are approximately equal. Also, the

cross-sections of 160 and 420 m have similar rates of settlement. Similarly, the points installed in central cross-sections of 260 and 360 m provide a similar pattern of settlement. Except for a few points such as S03, S53, S54, and S55 that have a small value of the settlement and seems that have reached a stable condition, all other points still have large quantities of settlement (see part 5.1). These points with low rates of the settlement are located at side sections of the downstream shoulder, where the height of the fill embankment is smaller than other parts of the dam.

With the assessment of the settlement pattern of points on the downstream embankment (Figures 4c-e), we infer that the points on the cross-section of 360 (i.e., points S33, S34, and S35) have the maximum values of settlement, whereas the points of Section 260 (i.e., points S23, S24, and S25) show lower settlements. In other words, the northern part of the dam from Section 260 to the spillway has experienced more settlement than the southern part of the embankment of the dam (from the left support to cross-section 260). This differential movement has caused several cross and longitudinal cracks on the crest that was observed at our field visit (Figure 2). One reason for this deformation and the presence of these cracks could be the discontinuity between the embankment and concrete spillway and the high slope of the spillway that caused the downward movement and creep of the spillway.

Table 6. 3D displacement of target points of the Masjed-Soleyman dam from Dec. 2000 to May 2015. D is the horizontal displacement; a, b, and az represent the dimensions and azimuth of the semi-major axis of error ellipse; $\sigma_{\Delta Z}$ shows the standard deviation of height differences.

Target Points	ΔX (mm)	ΔY (mm)	D (mm)	a (mm)	b (mm)	az (deg)	ΔZ (mm)	$\sigma_{\Delta Z}$
S01	-261.88	466.09	534.62	3.7	1.2	119	-816.59	1.7
S02	-380.67	440.28	582.03	4.4	2.8	35	-824.46	1.7
S11	-480.07	745.1	886.37	2.9	1.9	144	-1776.48	1.7
S12	-376.13	692.79	788.31	2.7	2.4	135	-1614.89	1.7
S13	-722.93	118.6	732.6	3.4	3.2	173	-793.89	1.8
S21	-639.35	459.33	787.24	2.8	2.5	147	-3525.96	1.7
S22	-684.11	343.06	765.31	2.7	2.4	153	-3326.15	1.7
S23	-1396.9	-196.84	1410.7	3.5	3.2	149	-1205.96	1.8
S24	-785.38	-81.13	789.55	3.2	3.0	134	-824.43	1.9
S25	-109.46	6.8	109.67	3.0	2.9	132	-64.06	2.0
S31	-119.74	-630.83	642.09	2.9	2.8	96	-3246.3	1.7
S32	69.1	-599.5	603.47	2.9	2.8	124	-2783.76	1.7
S33	-1322.38	-246.08	1345.08	3.4	3.0	141	-1246.4	1.7
S34	-767.31	-126.92	777.74	3.3	2.9	136	-994.47	1.9
S35	-155.73	-31.4	158.86	3.2	2.8	134	-191.48	2.0
S41	-126.93	-889.8	898.81	3.1	2.9	116	-1956.86	1.7
S42	-15.88	-806.13	806.29	2.9	2.6	133	-1707.05	1.7
S43	-879.25	-366.58	952.61	3.4	3.0	127	-894.64	1.7
S44	-505.68	-256.8	567.15	3.4	3.0	146	-567.31	1.9
S45	-88.11	-50.39	101.5	3.2	2.9	144	-106.75	2.0
S51	-158.62	-725.61	742.75	3.0	2.6	114	-1033.5	1.7
S52	-120	-676.55	687.11	2.9	2.5	132	-947.28	1.7
S53	-263.98	-276.39	382.2	3.3	2.5	146	-286.68	1.8
S54	-8.95	-27.72	29.13	5.6	3.9	135	-2.49	1.9
S55	2.06	-16.9	17.02	5.0	3.8	133	-9.57	2.0
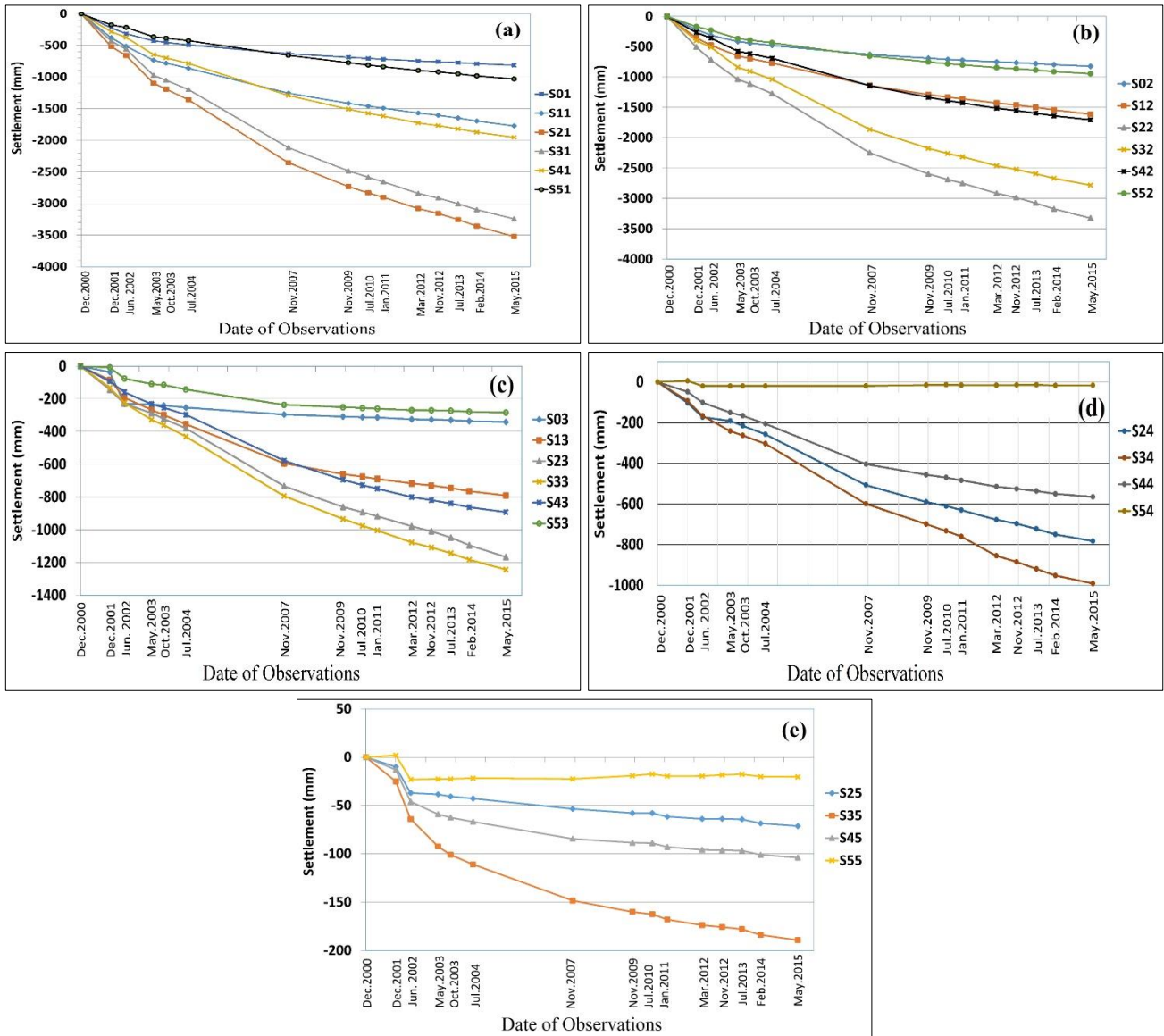
Figure 4. Settlement of target points of the Masjed-Soleyman dam derived from 15 sets of terrestrial geodetic measurements; (a) points of the upstream edge of crest, (b) points of downstream edge of the crest; (c) & (d) and (e) points installed on the downstream slope at elevations of 347 m, 310 m, and 270 m, respectively.

Figures 5a&b shows the settlement pattern for the upstream and downstream sides of the dam crest. It is seen that the behavior of both patterns is approximately similar. It can be seen that the crest has had a convex form before the impoundment of the reservoir and because the settlement has changed to a concave form over time. Figures 5c-d show the settlement of target points during three steps of dam operation time: The first year of dam operation, 3rd year of dam operation (when the reservoir of the dam was approximately filled) and after 15 years of dam operation. As figures show, the settlement of the middle part of the crest is very greater than that of other parts. Also, the settlement of side points and the lower part of the embankment are very small during dam operation.
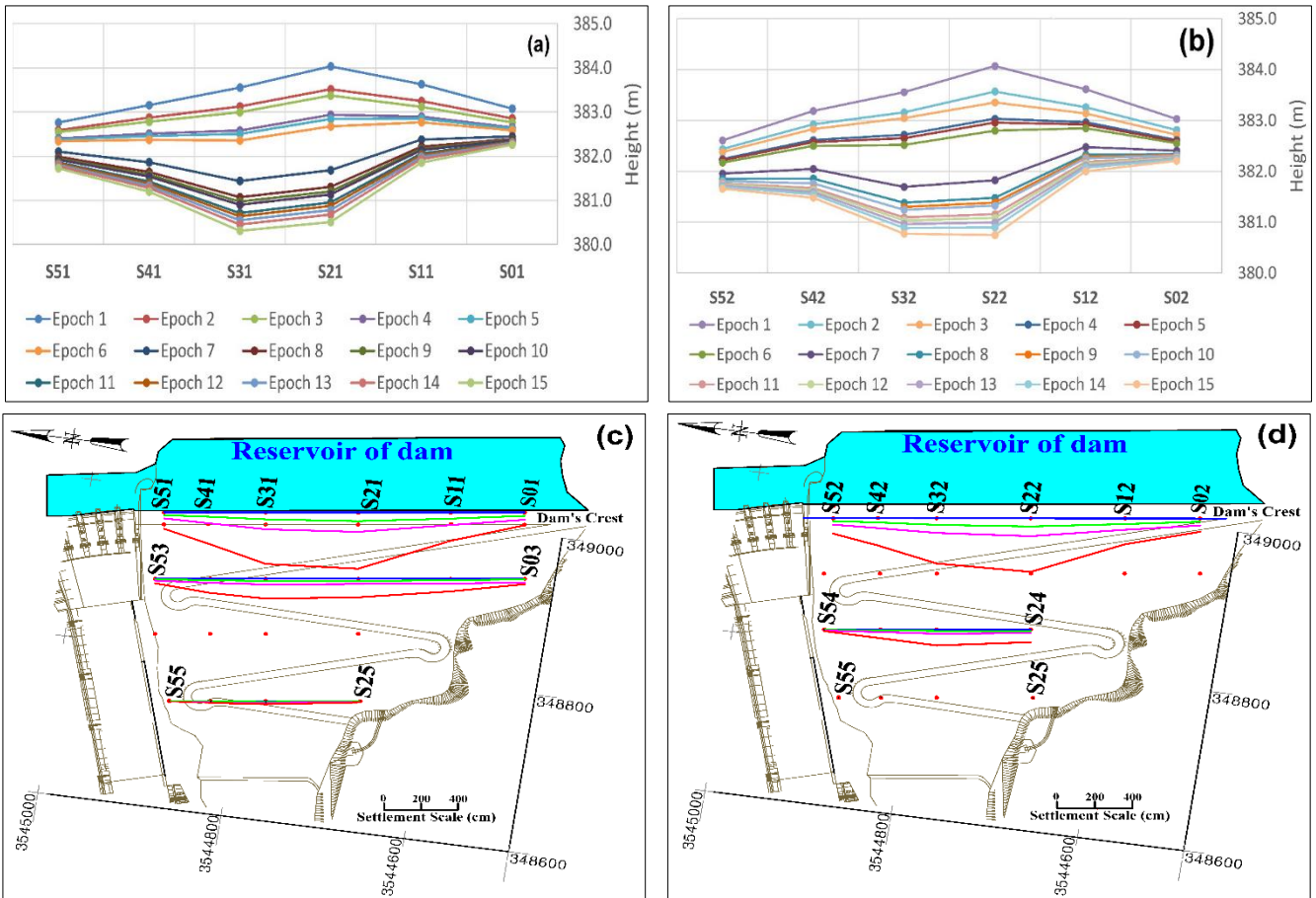
Figure 5. Changes in the heights of the points located on the crest points during 15 terrestrial observations. (a) Upstream edge of the crest; (b) downstream edge of crest; (c &d) settlement of points during three steps of dam operation:1st year (green line), 3rd year (magenta line), and 15th year (red line) after impoundment of the dam.
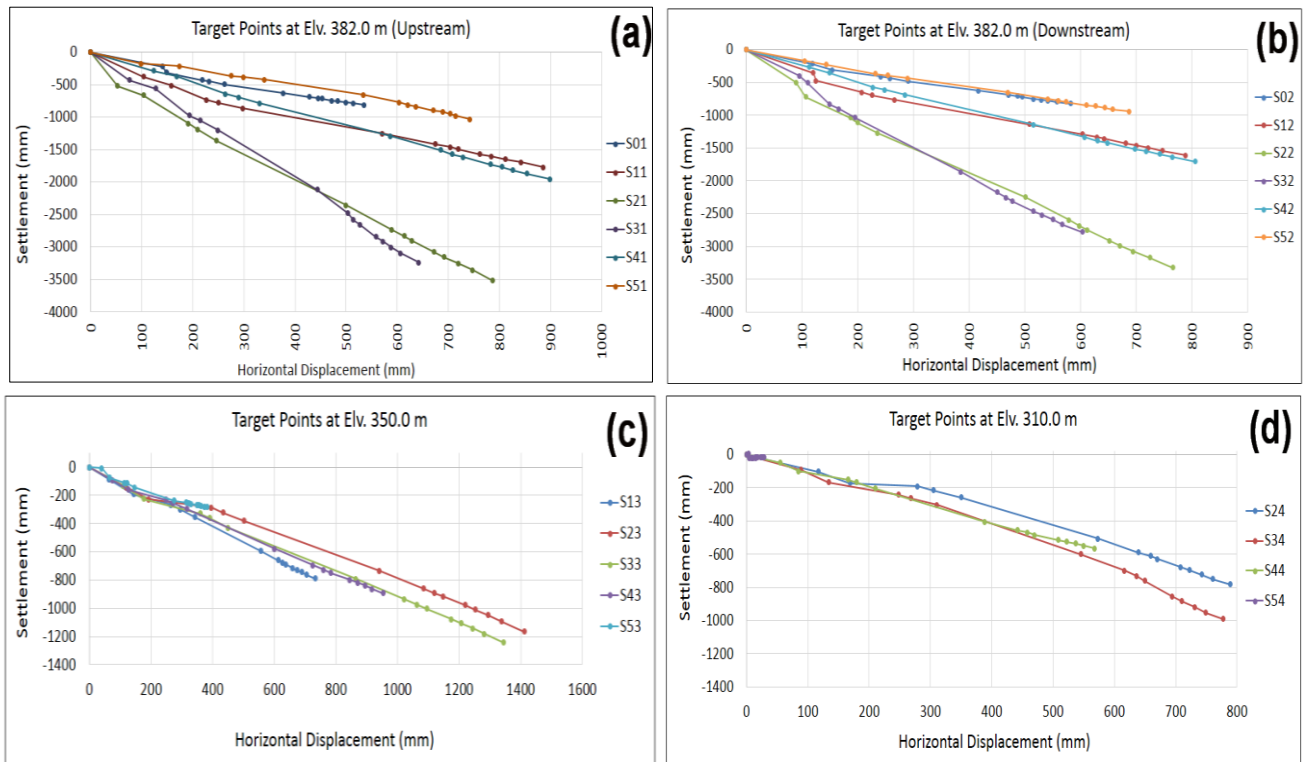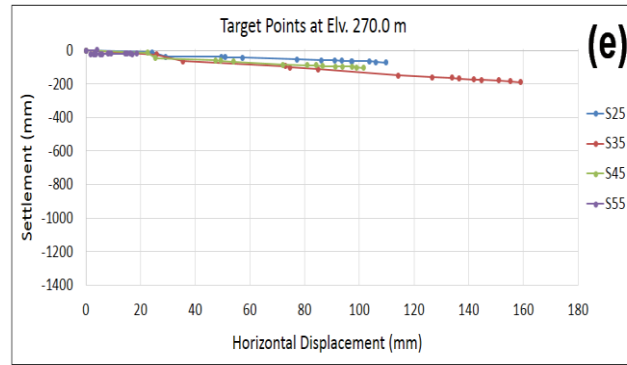
Figure 6. Vertical /horizontal displacement of target points located on the crest and downstream slope of the dam. (a), (b) displacement of points installed on the upstream and downstream edge of crest, respectively. (c), (d) and (e) show the displacement for points located at the downstream slope in elevation of 350 m, 310 m, and 270 m of the dam embankment, respectively.

3.2. Horizontal Displacement

Horizontal deformations are common in earth-fill dams after construction and during the operation. Since there are not any control points installed on the upstream embankment of the dam, the analysis of this part of the dam was not possible by the existing dataset, but site visit revealed that the upstream slope had moved toward the east that could be a result of creep of the embankment of the dam (Figure 2a).

Figures 7a-c present the horizontal displacement of target points installed on the dam's crest and downstream embankment of the Masjed Soleyman dam. As figures show, the direction of movements for points located on the crest of the dam is toward the middle and downstream of the dam. It seems that this movement has resulted from the high slope of the side supports of the dam, especially for the right support of the dam, where the downstream embankment is connected to the concrete spillway. The slope of lateral supports is 1/1.19 and 1/1.38 for right and left supports, respectively (Figures 1b). However, some points located on the left part of the crest have moved toward the upstream direction of the dam for the first stages of filling the reservoir (Figure 7a). The maximum horizontal displacement in this step belongs to the point S01 (Figure 3b) with a magnitude of 141 mm. The upstream movement of the crest is potentially originated by the hydrostatic pressure from the reservoir, causing the submerged part of the dam to deform towards the downstream direction, but at the same time resulting in an upstream movement of the crest (Michalis & Pytharouli, 2016).

It should be pointed that this is not true for the horizontal deformations of the object points located on the downstream embankment, and these points have moved downward, as illustrated in Figures 7a-c.

Figure 7b shows the cumulative horizontal displacement of points of this network after the third year of dam operation in 2003, corresponding to the 5th series of geodetic measurements of the dam. The maximum displacement of points with respect to the 1st period belongs to the point S23 with a magnitude of 434 mm. This point is located in Section 260 in the middle part of the dam, with a height of 347 m.

After the observations, points S23 and S33 showed a horizontal displacement of 1410 mm and 1345 mm, respectively. On the other hand, the maximum horizontal displacement for points S21 and S31 located in the middle part of the dam crest, which has the maximum settlement, are 787 and 603 mm, respectively (Figure 7c). In other words, the points located at the elevation of 347 m have the maximum horizontal displacements, while the points located at the center of the crest have the maximum settlement. Thus, this horizontal movement could have resulted from the collapse of the downstream slope caused by the steep slope of side supports and the improper consolidation of the earth layers during the dam construction (Emadali, L, Motagh, M, & Haghshenas, M, 2017). As shown in Figure 2a, the collapse phenomena are also observed for the upstream embankment. However, as there were no control points on the upstream slope, we could not infer any information on the status of the horizontal displacement for this part of the dam body.
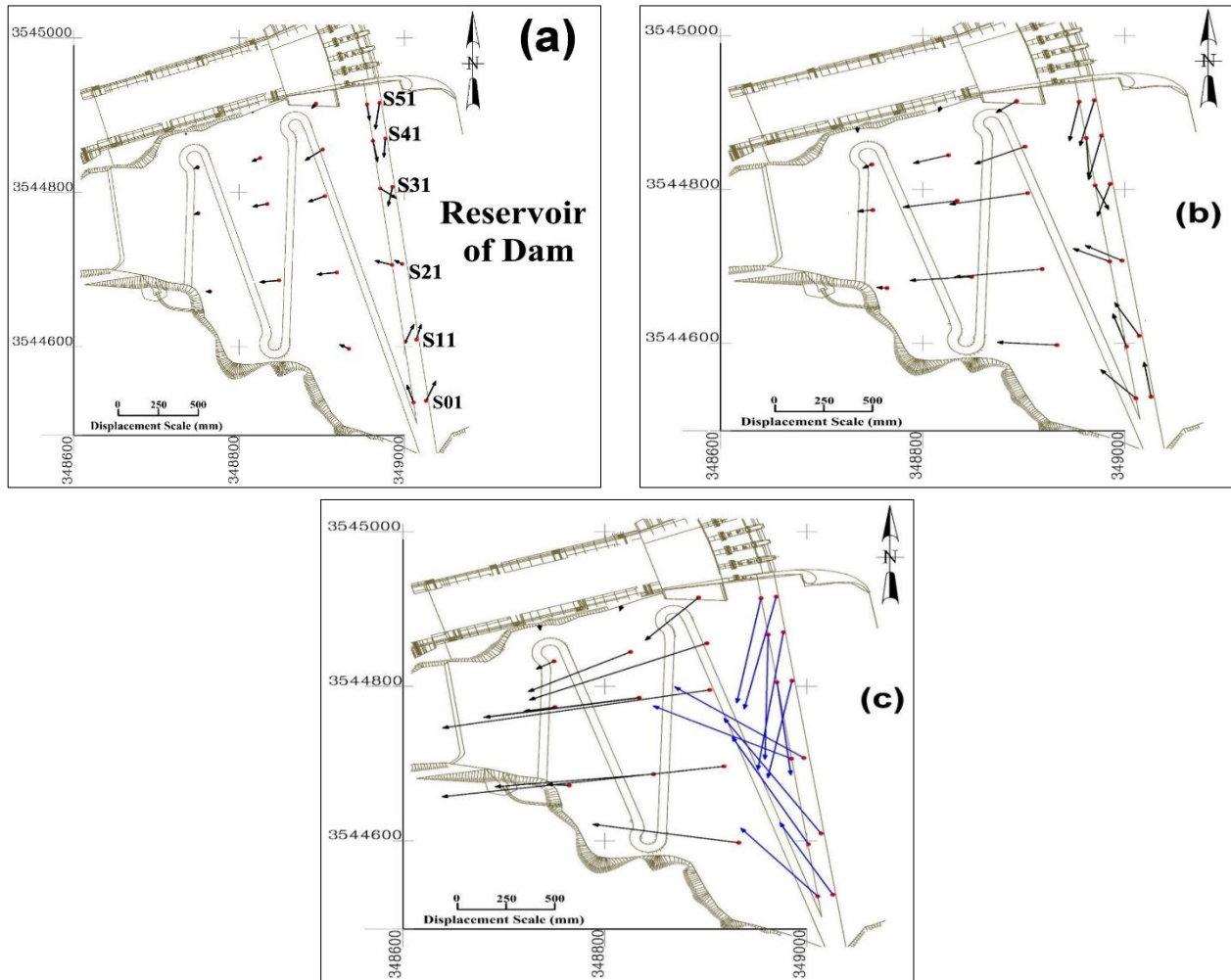
Figure 7. The horizontal displacement of object points installed on dam body; (a) during the first year of dam impoundment, (b) three years after the dam operation, (c) after the 15th year of dam operation.

3.3. Rate of Settlement

The settlement reflects the compressibility of the core, and the relatively high settlement values could possibly be explained by the lack of compaction at the placement stages of construction (Dascal, 1987). In the Masjed-Soleyman dam, the level of water increased rapidly and changed from 254.8 m on 19 Dec. 2000 to 305.7 m on 31 Dec. 2000 (1st period of surveying measurements). Then, the water level raised and reached 369.35 m on Oct. 2003 (5th period of surveying measurements). This means that the water level increased by about 114.5 m in the time duration of 34 months (Emadali, L, Motagh, M, & Haghshenas, M, 2017). Afterward, the water level has experienced fewer fluctuations which are related to this type of dams, constructed mainly for power generation (Run-off-the-River dams). Accordingly, the settlement of the dam was assessed in three separate steps. At first, the settlement of the dam was evaluated for the first year of operation (December 2000 to December 2001). Then, the settlement was assessed for the first three years of water impoundment from December 2000 to October 2003, during which the reservoir has almost been filled. Finally, the rate of the

settlement was evaluated for the total time of operation of the dam from December 2000 till May 2015.

For the first year of water impoundment of the Masjed-Soleyman dam, point S21 installed on the upstream edge of the crest has the maximum rate of settlement. This point has experienced a settlement rate of ~ -52 cm/yr during October 2000 till October 2001. Also, other points close to point S21, such as S22, S31, and S32, had large values of settlement. These values are not far-fetched because these points have been established in the middle part of the dam's crest that has the maximum height of the embankment. At the same period, point S55, which is located at the lower part of the side cross-section of the dam, with the minimum height of embankment (Figures 3a & 9a), had the minimum rate of the settlement with a magnitude of -2 mm/yr.

The maximum settlement rate for the first three years of operation of the dam (the time of filling the reservoir) from December 2000 to October 2003 was ~ 41 cm/yr, corresponding to the point S21 on the crest (Figure 3a). From October 2003 to November 2007, the water level reached the maximum value, and the reservoir was filled. In this period, the rate of settlement decreased and reached to

about 35 cm/year for point S21. From November 2007 to May 2015, the water level had no significant changes. Consequently, the rate of the settlement was diminished and reached ~ 16 cm/yr. If one considers the total settlement of point S21 during 15 years of dam operation, the mean rate of settlement is ~ 25 cm/yr. The maximum cumulative settlement of the points installed on the dam is ~3.5 m that corresponds to the 1.99 % of the maximum height of the dam.

It is worth noting that the first period of surveying measurements was done simultaneously with the filling the reservoir. Thus, the settlement after the completion of the structure and before the water impoundment of the reservoir is neglected. This part of the settlement is caused by reducing the pore water pressure of the clay core, known as primary consolidation. To determine the magnitude of the settlement before the water impoundment, the observations of settlement gauges installed at different levels of core were evaluated. The topmost settlement gauge at section 260 m, which has been observed before the filling of the reservoir, installed at the elevation of 373.435 m. This instrument shows the settlement of about -48 cm in the time duration of 23 Sep. 2000 and 20 Dec. 2000 (start date of filling the reservoir). This value should be added to the total settlement of the dam for the point of S21. According to this, the average settlement rate of point S21 during 15 years of operation is about 28 cm/yr. The total settlement of

this point reaches ~ 4 m, corresponding to 2.26 % of the maximum height of the dam, while the maximum settlement of an earth/rockfill dam should be smaller than 2 % of the height of the dam during its operation (Kaloop, 2009).

3.4. Settlement Index analysis

Figures 8a and 8b show the S_I parameter for the object points installed on the dam's crest and on the downstream embankment of the Masjed-Soleyman dam during the 15 years of terrestrial geodetic observation. As Figure 8a shows, some target points in the middle section of the dam (Sections 260 & 360), such as S21, S31, S22, and S32, exhibit settlement index SI that exceeds the threshold value of 0.02. This indicates that for these points, the deformation of the dam embankment is critical and cannot be attributed only to the normally expected phenomenon of soil creep (Michalis & Pytharouli, 2016).

The points S23 and S34 (Section 260 & 360 from Figure 3a), show S_I parameters that are close to the critical limit (0.0168 for S23 and 0.0191 for S34). However, other target points installed on the downstream slope show S_I values less than the threshold of 0.02 (Figure 8b). This suggests that for the downstream embankment, one can attribute the deformation to the normal creep of the dam.
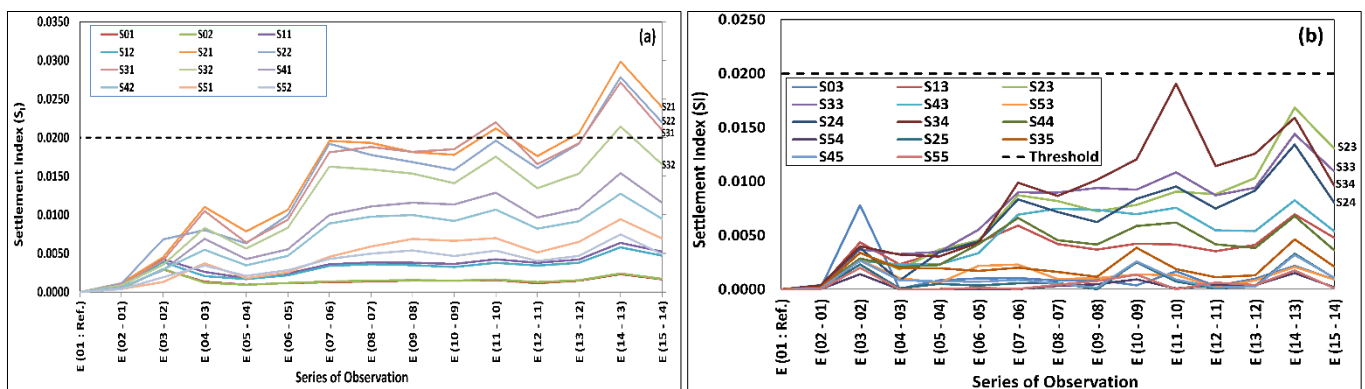
Figure 8. Settlement Index (S_I) for geodetic points on the (a) crest and (b) downstream embankment during 15 series of geodetic observations. The dashed black line offers the critical value of 0.02.

Figures 9a and 9b show the annual rate of settlement for all points installed on the crest and downstream slope of the dam, respectively. As can be seen, after the 12th year of dam operation, the rate of settlement for the majority of the crest points has decreased to the normal threshold (lower than 0.02%). However, one year later, an ascending trend is seen for most of the points on the crest. On the other hand, for the points on the downstream slope, the annual rate of settlement gets values smaller than the threshold after the

10th year (except for point S34 that shows an increasing trend between the 10th and 12th years and again decreases to the threshold limit). Also, the points S23 and S33 show an increasing trend after the 13th year of dam operation. These points are located in the middle part of the dam body (Figure 3a). Other points of the dam body are in the normal range, which means these points experience stable conditions.
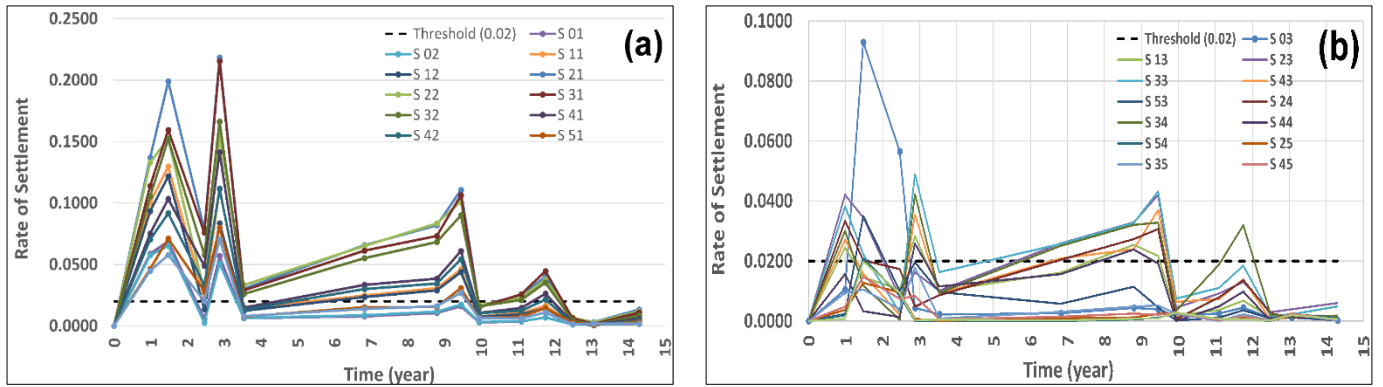
Figure 9. The annual rate of settlement for points of the on-dam network; a) crest points; b) points installed on the downstream embankment of the dam. The Dashed line shows the threshold limit of 0.02 %.

3.5. Relaxation Model

It is difficult to link specific processes with specific relaxation times for post-construction deformation. There can be a wide range of relaxation times consistent with a specific process, and it is likely that the processes overlap in time, perhaps operating simultaneously for a significant period (Massiéra, Chrzanowski, Anna Szostak, & Michel , 2004). Table 7 represents the estimated quantities for seven parameters of the relaxation model. We estimated a model for all points installed on the crest and downstream embankment of the dam (on-dam Network).

According to the results obtained from settlement analyses (rate of settlement, settlement index, and relaxation model),

the on-dam geodetic network was divided into four deformation zones (Figure 10). For this partitioning, the points were arranged based on their settlement during 15 years of dam operation, as follows:

- Zone 1 (Green):   points with settlement < -1000 mm

- Zone 2 (Yellow): $-2000 <$ settlement < -1000 mm

- Zone 3 (Blue): $-3000 <$ Settlement < -2000 mm

- Zone 4 (Red): $-6000 <$ Settlement < -3000 mm

Table 7. The estimated parameters of the model for the five zones (zones 1 to 4 and crest points)

Point Id.	a (mm)	b_1	b_2	b_3	τ_1 (day)	τ_2 (day)	τ_3 (day)	RMSE (mm)	R^2
S01	-1090	514.6	140.5	618.9	319.2	2702	6048	3.971	0.9998
S02	-1076	553.3	223.3	575.9	247.5	2437	5801	3.739	0.9998
S03	-444.2	1384	-102.1	285.4	184.6	1095	4838	17.6	0.9701
S11	-2573	-22910	23210	2177	1110	1095	5432	18.84	0.9992
S12	-2234	547.7	683.7	1266	201.8	2723	6144	13.74	0.9995
S13	-876.7	241.8	890.8	0.3953	180.2	2349	5124	14.98	0.998
S21	-5698	-1715	3080	4135	703.5	1160	8301	47.12	0.9990
S22	-4070	-240	4231	-99.21	644.5	3260	8150	47.9	0.9988
S23	-1824	-313.9	405.8	1625	590.2	1299	5975	22.84	0.9979
S24	-1045	-428.8	478.8	896	786.3	1482	4189	18.12	0.9971
S25	-91.86	61.29	-48.47	91.62	231.7	1095	3652	2.495	0.9862
S31	-5156	-255	1615	3748	755.9	1855	7344	41.25	0.9991
S32	-4073	-1765	3051	2639	914.3	1416	6952	34.43	0.9992
S33	-1753	-136	692.9	1177	859.4	2549	5237	14.99	0.9992
S34	-1498	401	-456.6	1854	180	1297	4055	17.81	0.9984
S35	-226.7	313	59.72	110.6	197.1	2090	4521	1.867	0.9993
S41	-2705	252.8	2408	138.8	365.4	4228	6464	24.07	0.9991
S42	-2502	490.4	153	1817	2209	1095	5958	20.31	0.9992
S43	-1041	-380.5	1552	-177.9	865.3	2614	4680	12.76	0.999
S44	-715.4	-155	512.2	359.5	552.3	1615	5182	11.6	0.998
S45	-121.8	330.5	-20.79	88.13	180	1095	3455	1.771	0.9964
S51	-1800	230.1	-414	2037	391.4	4370	6382	14.42	0.9988
S52	-1293	255.2	856.1	271.3	352	4003	6440	9.994	0.9993
S53	-286.9	-19060	424	19220	314.3	1278	310	7.939	0.996
S54	-20.96	271.9	-35.64	15.82	181.6	1095	4530	2.624	0.9134
S55	-23.98	207.9	-30.29	16.92	180.5	1166	3774	2.594	0.9075

Figure 10. Four zones of settlement in the Masjed-Soleyman dam. Green, yellow, blue, and red blocks represent the zones 1, 2, 3, and 4, respectively. The red block (zone 4) represents the maximum settlement, and the green block (zone 1) represents the minimum settlement of points.

Figures 11 (a-d) represent the time series of observed data and relaxation function for the points in zones 1 to 4, respectively. As expected, the relaxation coefficient, τ_3, for the model of points located in the middle part of the crest was much greater than that of the other points. Moving toward the lower parts of the embankment, the value of this parameter decreases.

The maximum RMS of points belonged to the points S22, S21, S31, and S32 in the middle of the dam with a magnitude of 47.90, 47.12, 41.25, and 34.43, respectively. The R^2 values for all target points, except for the points S03, S54, and S55 were greater than 0.99, presenting a good fitness of the model to observed data. For these three points, the R^2 values were greater than 0.91. According to these models, the settlement of the dam for the most points would still continue even to about 30 years of dam operation. For example, the settlement of points S21 and S22 in the middle of the crest will reach about 4 m or more that would exceed the maximum acceptable settlement for this dam. However, it seems that the points located at the bottom of the downstream embankment (points located at the black rectangle in Figure 3b) and some points located at the sides (near the staddles such as S03, S53 & S54) have already reached to stable conditions (Stewart & Tsakiri, 2001).
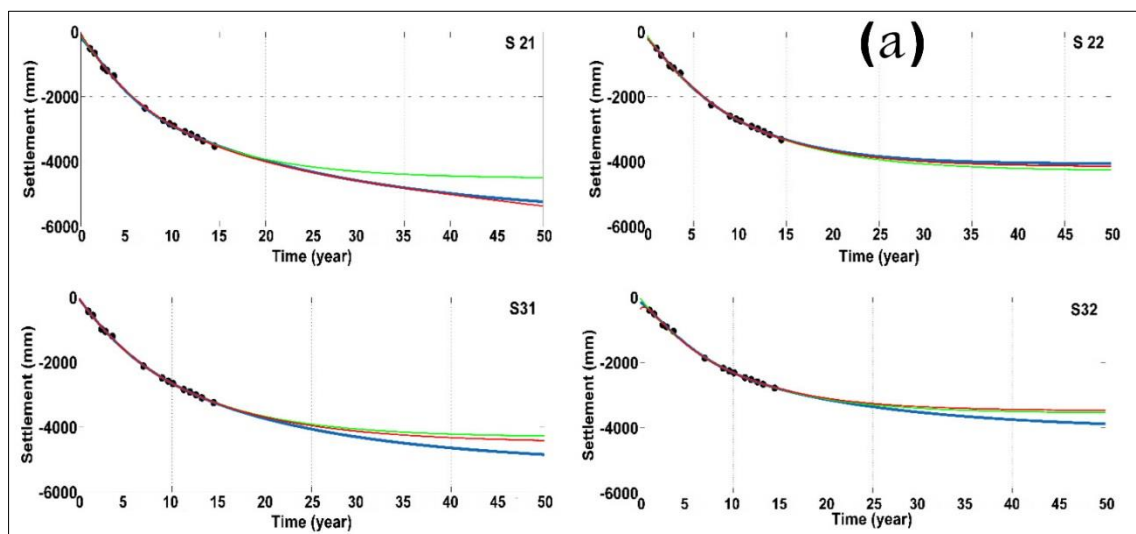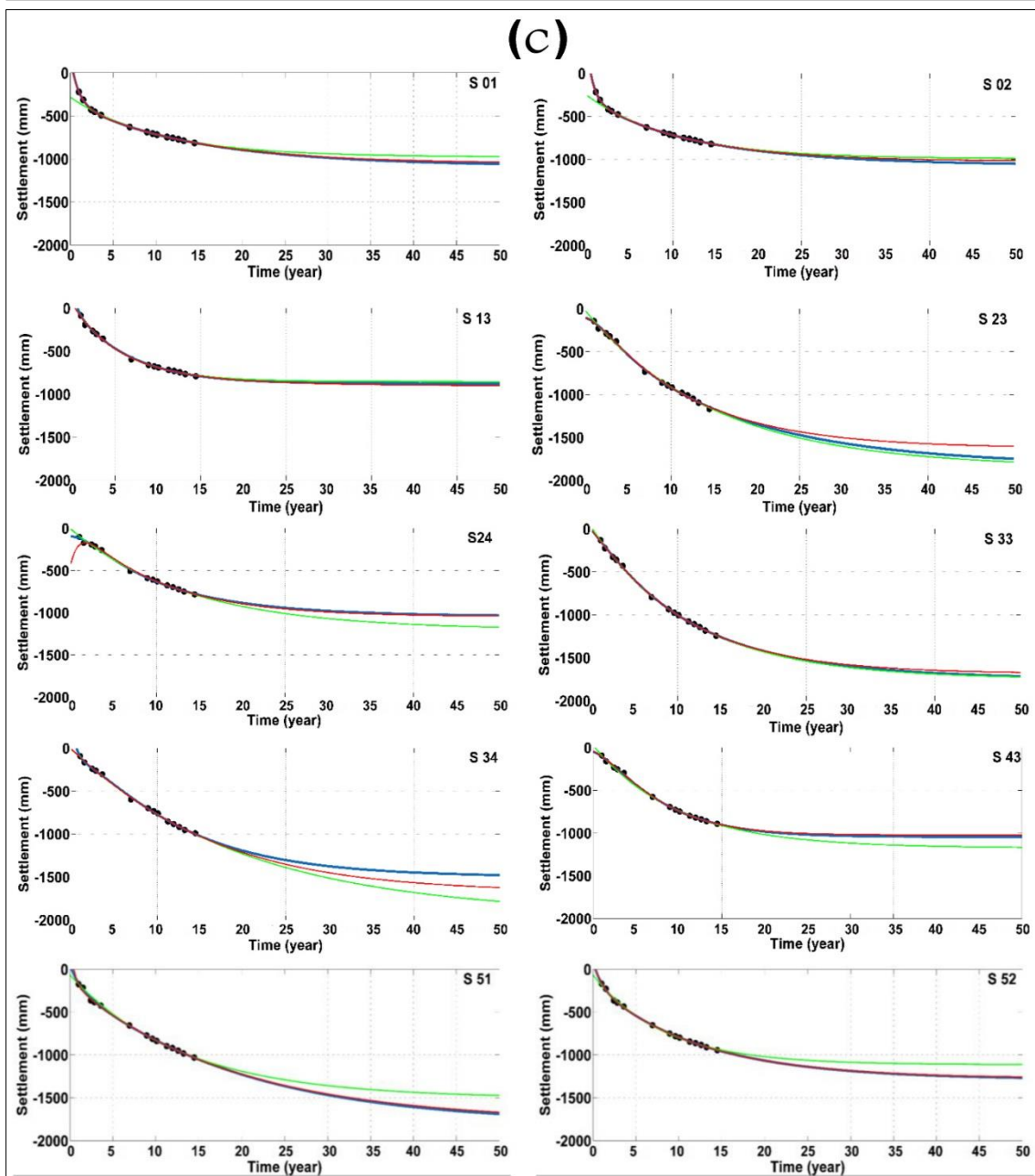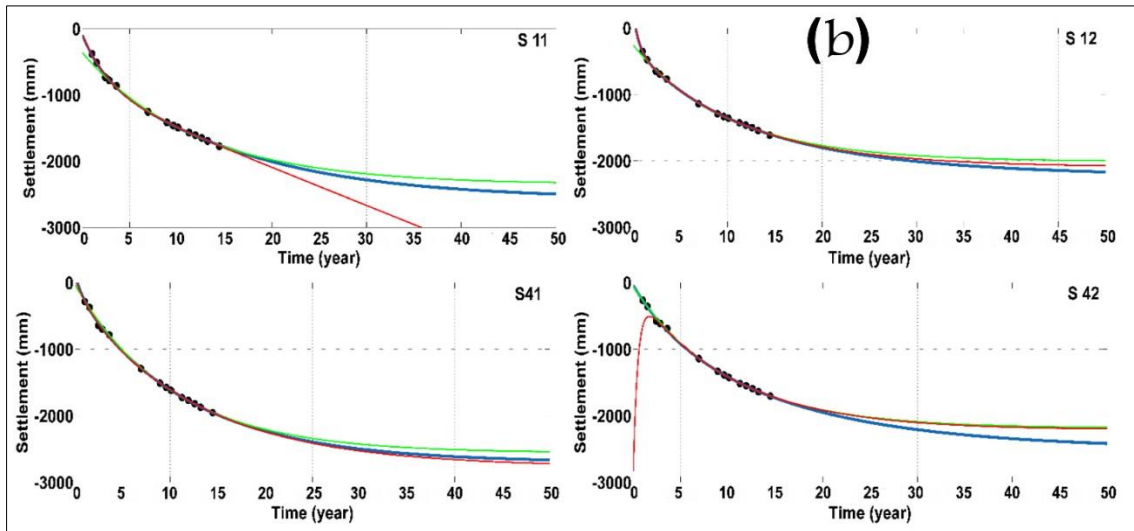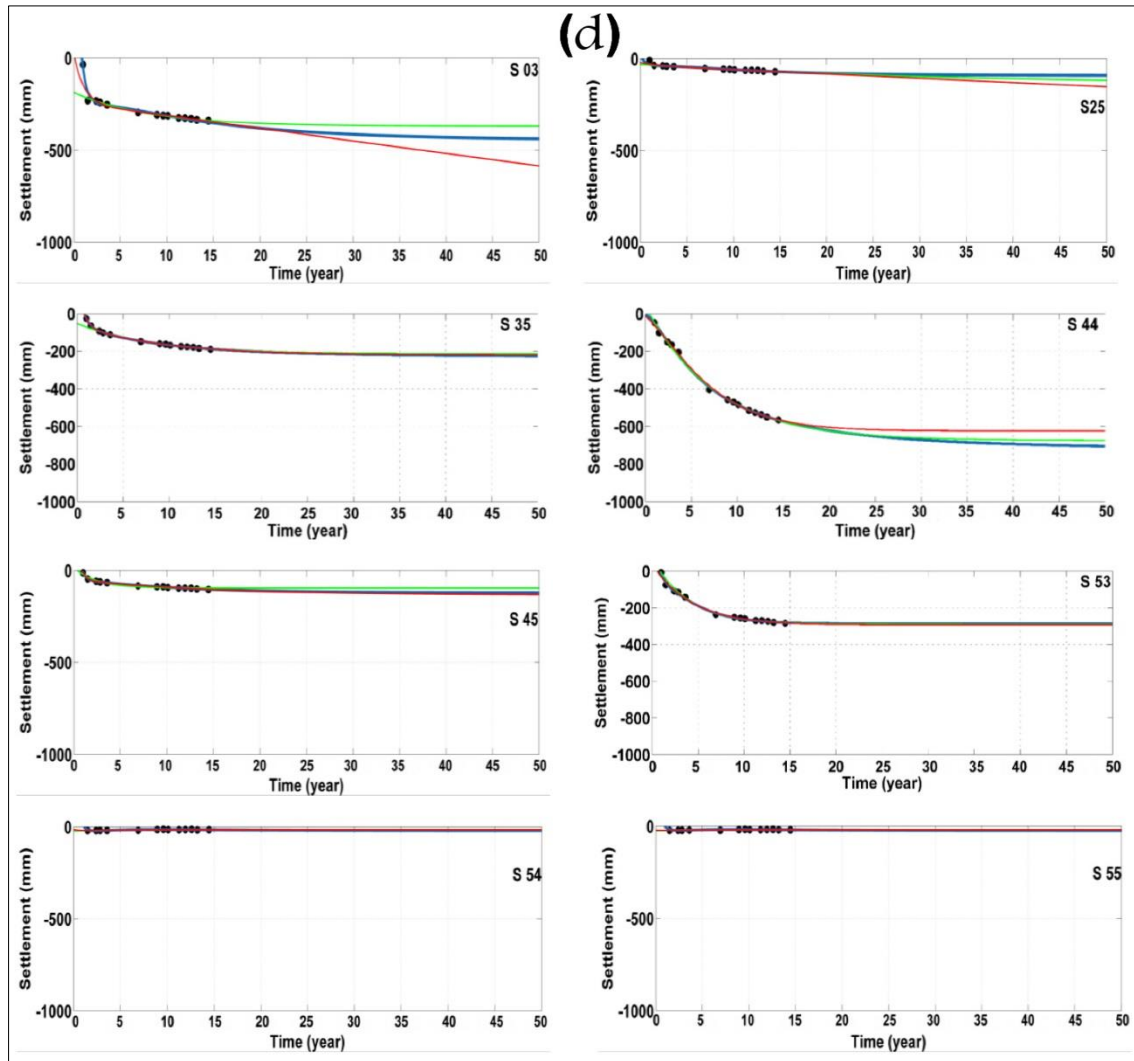
Figure 11. (a-d) Time series of the settlement of object points installed on the dam body during operation by use of 15 years surveying dataset from 2000 to 2015 and relaxation model for prediction of vertical displacement of the dam until 2050: (a-d) for the zones 4 up to 1, respectively.

It can be seen from Table 7 that:

(1) The value of parameter τ_1 for point S42 is greater than the other points. The reasons for this can be the proximity of this point to the steep slope of the right support and the vicinity of section 420 m to the concrete spillway of the dam. This is supported by the large settlement observed at the conjunction point of the spillway, proved by the dam embankment (Figure 2). The next reason may be attributed to the high elevation of the embankment at this point (about 100 meters).

(2) Regarding τ_2, the maximum values are also related to the points located in the sections of 420 and 480 m (Figure 3a) such as the points S41 and S51 located on the upstream edge of the crest of dam. This could be due to the effect of filling the reservoir.

(3) As expected, the highest values of τ_3 are related to the points located in zone 4 (the points installed in the middle of the crest, including S21, S22, S31, and S32). Also, the values of this parameter for other points located on the crest of the dam show larger quantities than the points of the dam body, indicating the secondary consolidation of the dam and the effect of the height of the embankment on the subsidence of these points.

(4) The maximum total relaxation times belong to points S22 and S21 in about 33 and 28 years, respectively, because of their positions in the middle of the dam and also the height of the embankment at these points. The points S41 and S51 located on the north of the dam's crest show a relaxation time of about 30 years, which seems relatively unreasonable.

4. Discussion

It is relatively straight-forward to monitor the settlement of the crest of an embankment dam using precise surveying

techniques. It is not always easy to interpret the measurements and diagnose the cause of the settlement, as it may occur due to a number of processes (Charles, 1986). The main processes are:

(1) Primary consolidation of clay
(2) Volume reduction of the upstream fill on first filling
(3) Secondary compression of core and shoulder fill
(4) Slope instability
(5) Erosion

Settlement due to cases 1 and 2 should be completed during the early years of the dam's life. It is clearly important to determine whether settlements measured many years after the completion of a dam can be attributed to case 3 or whether serious problems such as cases 4 or 5. To do this, some indication of the magnitude of the crest settlement should be obtained (Cazzaniga, Pinto, Bettinali, & Frigerio , 2006). One of these indicators is the settlement index (S_I).

The deformation of the rockfill and earthfill dams continues for a long time after the end of construction. However, considering that an annual rate of settlement below 0.02 % H can practically be neglected, deformation can be considered complete 24 – 30 months after the end of construction. Figure 8 shows that the rate of horizontal and vertical displacement has not diminished for most of the points of the on-dam geodetic network during 15 years of the dam operation. Except for a few points at the bottom of the downstream slope of the dam (zone 1), displacement of all other points still continues.

The results of our analysis suggest that the points located at zone 4 in the middle part of the dam's crest represent the maximum settlement in the time duration of 2000 to 2015. These points also have the maximum relaxation times during the dam operation, i.e., the coefficient τ_3 in Eq. 3 (Tab. 7). This results from the maximum height of embankment in these points located at the cross-sections of 260 and 360 m (Figures 3a&b). In zone 3, although the rate of settlement has decreased compared to zone 4, the great values of settlement can be seen for some points, such as point S41 with the settlement of about 2.0 m during 15 years of dam operation. In zone 2, smaller settlements have been measured (maximum settlement for point S33 is about 1.25 m), but the maximum horizontal displacement in this zone belongs to point S23 with a magnitude of about 1.4 m. Points in zone 1 have the minimum settlement with respect to other points of the network, and thus, this part of the dam could be considered as an area that has been reached to the stable conditions. As the settlement index analysis shows, the maximum values of the index for these points reach about 0.005 (Figures 8b). InSAR analysis of TerraSAR-X images also confirms the stability of this zone (Emadali, L, Motagh, M, & Haghshenas, M, 2017).

The relaxation time modeling of points showed that the settlement of the dam might be continued even 30 years after the end of the construction of the dam. The mean annual rate of settlement during the next 15 years of dam operation (from 2015 to 2030) would be estimated to about -71 mm/yr for point S21 in the middle of the crest. From 2030 to 2040, the mean rate of settlement of point S21 would reach to about -39 mm/yr, and for the following ten years (2040 -2050) to about -25 mm/yr. At that time, the cumulative settlement of point S21 (maximum settlement of the dam) would be more than -5 m that is a great amount and exceeds the threshold of 2% of the dam's height.

Also, according to the suggested model, point S22 in the middle of the dam may get the maximum relaxation time of about 33 years. As discussed in 3.5, some other points such as S41 and S51 would experience the great relaxation times of about 30 years, as well. Point S22 would get a relaxation time of about 27 years. However, these great values for the relaxation time of a rockfill dam are not normal. They show continuous settlement of the dam even for 30 years of dam operation, which poses a great hazard to the people and infrastructure downstream. The worrying point about the presented relaxation model in this paper is that it is not unique. However, according to the available data, the proposed model has proved useful for interpreting the results obtained from geodetic observations.

5. Conclusion

In this paper, we analyzed the deformation of the Masjed-Soleyman rockfill dam in southwest Iran based on 15 terrestrial observations made for the geodetic network on the dam embankment between 2000 and 2015. Our analysis indicates that 15 years after the first water impoundment of the dam's reservoir, most parts of the dam have not experienced stable conditions. Previous studies suggest that in normal cases, a dam should reach the stable condition (i.e., annual settlement rate less than 0.02%) over 8-10 years (Clements, 1984). The most important reason for the instability of the Masjed-Soleyman dam may be inappropriate consolidation of the upper layers of the embankment. Also, the fast performance of layers of the embankment, filling the reservoir immediately after the construction, as well as the steep slope of staddles and an improper junction of spillway and dam body may have contributed to this long-term instability. All these factors have caused numerous lateral and longitudinal cracks on the dam crest, especially where the concrete spillway is connected to the embankment, putting the dam safely at serious risk.

It is recommended that for future monitoring of the upstream shell of the dam, some target points be installed on this part of the dam so that their deformation can be

analyzed in more detail. Previous studies have also shown the importance of high-resolution SAR data for monitoring dam stability. Such data are not automatically acquired by satellite missions, and it is highly recommended that local authorities make such data acquisitions from space agencies for monitoring purposes (Emadali et al., 2017). Moreover, the development of a permanent GPS network containing some points on the crest can be a valuable add-on to the existing network and help with better monitoring of the deformation in time for areas that are at high risk.

References

Baarda, W. (1968). A Testing Procedure for Use in Geodetic Networks . *Netherlands Geodetic Commission, Delft, the Netherlands.*, vol. 2 No. 5.

Cazzaniga, Pinto, Bettinali, & Frigerio . (2006). : The Chimney of the Power Plant in Piacenza, Italy. *Structural Monitoring With GPS and Accelerometers*, (pp. 62-69). Austria.

Clements, & Ronald . (1984). Post-Construction Deformation of Rockfill Dams. *J. Geotech. Engrg*, 821-840.

Dascal. (1987). Post-Construction Deformation Of Rockfill Dams. *Journal of geotechnical engineering*, 73-92.

Dunnicliff, & John. (1988). *Geotechnical Instrumentation for Monitoring Field Performance.* Interscience publication.

Emadali, L, Motagh, M, & Haghshenas, M. (2017). Characterizing Post-Construction Settlement Of The Masjed-Soleyman Embankment Dam, Southwest Iran, Using TerraSAR-X Spotlight Radar Imagery. *Engineering Structures*, 261-273.

F, J. (2004). Dynamic Response of Masjed-Soleyman Rockfill Dam. *13th World Conference on Earthquake Engineering* (p. 987). Vancouver, B.C., Canada: B.C. Canada.

Gikas, Vassilis, sakellariou, & Michael. (2008). Settlement Analysis of the Mornos Earth Dam (Greece): Evidence from Numerical Modelling and Geodetic Monitoring. *Engineering Structures*, 3074-3081.

Hanssen. (2001). *Radar Interferometry, Data Interpretation and Error Analysis.* Kluwer Academic pablishers.

Kalkan, Y. (2014). Geodetic Deformation Monitoring Of Ataturk Dam in Turkey. *Arabian Journal of Geosciences*, 397-405.

Kaloop, M. R. (2009). Monitoring of Bridge Deformation Using GPS Technique. *ASCE Journal of Civil Engineer*, 423-431.

Massiéra, Chrzanowski, Anna Szostak, & Michel . (2004). Modelling Of Deformations During Construction of a Large Earth Dam In The La Grande Complex, Canada. *Technical Sciences*.

Massonnet, & Feigl. (1998). Radar Interferometry And Its Application To Changes In The Earth's Surface. *Reviews of Geophysics*, 441-500.

Michalis, & Pytharouli. (2016). Long-Term Deformation Patterns of Earthfill Dams Based On Geodetic Monitoring Data: The Pournari I Dam Case Study. *3rd Joint International Symposium on Deformation Monitoring*, (pp. 18-27). Vienna.

Milillo, Pietro, Perissin, Daniele, Salzer, Jacqueline , et al. (2016). Monitoring Dam Structural Health From Space: Insights From Novel InSAR Techniques And Multi-Parametric Modeling Applied To The Pertusillo Dam Basilicata, Italy. *International Journal of Applied Earth Observation and Geoinformation* , 221-229.

Pagano, L, Desideri, A, & Vinale, F. (1998). Interpreting Settlement Profiles Of Earth Dams. *J. Geotech. Geoenviron. Eng*, 923-932.

\Pytharouli, Stella , & Stathis . (2009). Investigation of the Parameters Controlling Crest Settlement of a Major Earthfill Dam Based on the Threshold Correlation Analysis. *Journal of Applied Geodesy* , 55-62.

Radhakrishnan, & Nisha. (2014). Application of GPS in Structural Deformation Monitoring: A Case Study on Koyna Dam. *Journal of Geomatics*, 113-124.

Rahimi, H. (2003). Embankment Dams. *university of Tehran Press*.

Savage, & Svarc. (2009). Post-Seismic Relaxation Following The 1992 M7.3 Landers And 1999 M7.1 Hector Mine Earthquakes, Southern California. *Journal Of Geophysical Research*, 63-77.

Shamshiri, Roghayeh, Motagh, Mahdi, Sharifi, Ali, M., et al. (2014). Deformation Analysis of the Lake Urmia Causeway (LUC) Embankments in Northwest Iran: Insights from Multi-Sensor Interferometry Synthetic Aperture Radar (InSAR) Data and Finite Element Modeling (FEM). *Journal of Geodesy*, 1171-1185.

Stewart, & Tsakiri. (2001). The Application of GPS to Dam Surface Monitoring. *Journal of geospatial engineering*, 45-57.

Vanicek, & Krakiwsky. (1986). Geodesy, the Concepts. *Elsevier Science Publishers*, 50 61.